The Matched Feedback Amplifier: Ultrawide-Band Microwave Amplification with GaAs MESFET's

KARL B. NICLAS, MEMBER, IEEE, WALTER T. WILSER, MEMBER, IEEE, RICHARD B. GOLD, MEMBER, IEEE, AND WILLIAM R. HITCHENS

Abstract—**An ultrawide-band amplifier module has been developed that covers the frequency range from 350 MHz to 14 GHz. A minimum gain of 4 dB was obtained across this 40:1 bandwidth at an output power of 13 dBm. The amplifier makes use of negative and positive feedback and incorporates a GaAs MESFET that was developed with special emphasis on low parasitics. The transistor has the gate dimensions 800 by 1 μm. The technology and RF performance of the GaAs MESFET are discussed, as are the design considerations and performance of the single-ended feedback amplifier module.**

I. Introduction

TWO-THIRDS of a century have gone by since, in 1913, Alexander Meissner was granted a patent on a feedback oscillator circuit by the German patent office. In the same year Edwin H. Armstrong presented a paper on regenerative circuits and in 1914 Lee DeForest, without whose earlier invention of the triode the feedback circuit would have been meaningless, filed a patent application on the regenerative circuit.

Ever since the invention of the original regenerative circuit, a great number of new feedback circuits with a multitude of applications have emerged. One particularly significant application is the use of negative feedback to control the gain and the input and output impedance of an amplifier [1]–[3]. It is, therefore, not surprising that the principle of negative feedback with its wide bandwidth potential, low input and output reflection coefficients, and good gain flatness has made its entry into the field of microwave amplifiers and, quite recently, into that of GaAs MESFET amplifiers [4].

This paper describes the use of both negative and positive feedback to extend the bandwidth of microwave amplifiers far beyond that reported to date. In order to accomplish this goal, a GaAs MESFET was developed with special emphasis on reduction of parasitics. Experimental amplifier modules exhibit a bandwidth of more than five octaves covering a frequency band from 350 MHz to 14 GHz. Minimum gain over this band is 4 dB at 13 dBm of output power. The amplifier makes use of "frequency controlled" feedback and simple matching techniques. The theory behind the basic feedback amplifier circuit is discussed in detail, as are the fabrication and performance of the amplifier modules. The technology, performance, and model of the GaAs MESFET are also described. Finally, gain, reflection coefficients, and reverse isolation of the computer model are compared to the measured data of two amplifier modules.

Manuscript received September 4, 1979; revised November 19, 1979.

The authors are with Watkins-Johnson Company, Palo Alto, CA 94304.

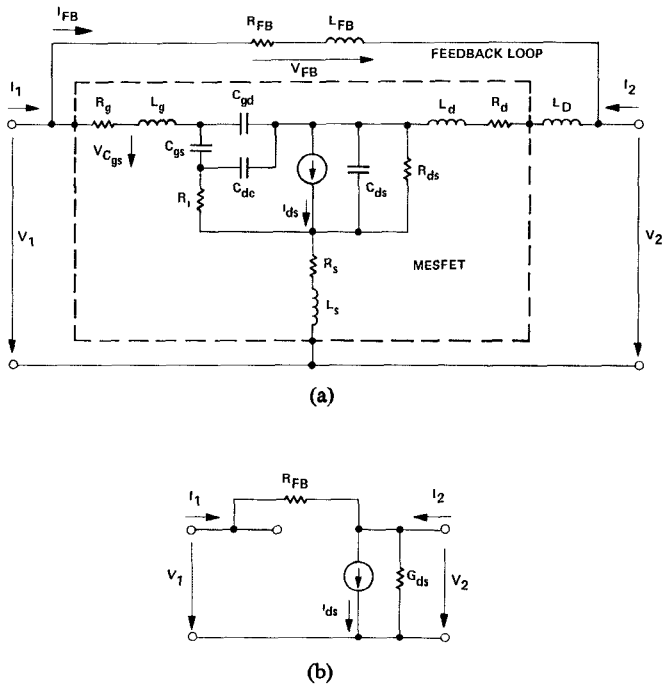

Fig. 1. Circuit diagram of the basic feedback amplifier. (a) High-frequency model. (b) Low-frequency model.

II. Basic Feedback Amplifier Circuit

The parasitic elements of a GaAs MESFET, as shown in the schematic of Fig. 1 (a), restrict the amplifier bandwidth capability. Minimization of these parasitics was a major goal of the device development, but there are obvious practical limitations. For this reason, we looked for supporting techniques to extend the bandwidth of the "conventional" negative feedback amplifier to higher frequencies. A practical answer was found in the introduction of the drain inductance L_D and the feedback induc-

0018-9480/80/0400-0285$00.75 ©1980 IEEE

TABLE I
ELEMENTS OF THE TRANSISTOR MODEL

INTRINSIC ELEMENTS		EXTRINSIC ELEMENTS	
g_m = 54 m mhos		R_g = 1.5 ohm	
τ_o = 3.5 psec		L_g = 19 nH	
C_{gs} = .67 pF		R_s = .9 ohm	
C_{gd} = .017 pF		L_s = .151 nH	
C_{dc} = .032 pF		C_{ds} = .082 pF	
R_i = 4.4 ohm		R_d = 2 ohm	
R_{ds} = 200 ohm		L_d = .143 nH	

DC BIAS CONDITIONS

V_{DS} = 4V

V_{GS} = -1V

I_{DS} = 100 mA

tance L_{FB}. These inductances and the parasitic elements of the GaAs MESFET are being employed to frequency control the feedback.

A. High-Frequency Model

The circuit diagram of the basic feedback amplifier making use of frequency controlled feedback is shown in Fig. 1(a). The amplifier's active device, the GaAs MESFET, is presented in form of its equivalent circuit, whose element values are listed in Table I [5]. The values of the reactive elements are small enough that at frequencies below 1.5 GHz all reactive elements can be neglected for determination of such quantities as gain, input and output VSWR and reverse isolation, i.e., up to 1.5 GHz the transistor can be represented by its dc model. However, the element values in Table I are such that aside from neglecting R_g, R_d, R_s, and maybe R_i, any further simplification of the high-frequency model of Fig. 1(a) leads to erroneous results at frequencies above 1.5 GHz. But even with $R_g = R_d = R_s = R_i = 0$, the admittance matrix of the basic feedback amplifier is so complicated that the computer provides the only efficient tool for obtaining solutions.

The basic feedback amplifier (Fig. 1 (a)) contains two series inductors, L_D in the drain line and L_{FB} in the feedback loop, that have been inserted to extend the amplifier's bandwidth. L_D was chosen to compensate for the capacitive portion of the output impedance at the upper band edge. It improves the output VSWR and eliminates the reactive component of the output impedance at this frequency. L_{FB} reduces the effectiveness of the negative feedback with increasing frequency.

The purpose of these two series inductors are best demonstrated by comparing their influence on insertion gain and bandwidth of the amplifier of Fig. 1. This comparison is presented in Fig. 2 for five selected combinations of R_{FB}, L_{FB}, and L_D. The curves clearly demonstrate the influence of L_D and L_{FB} on the bandwidth and

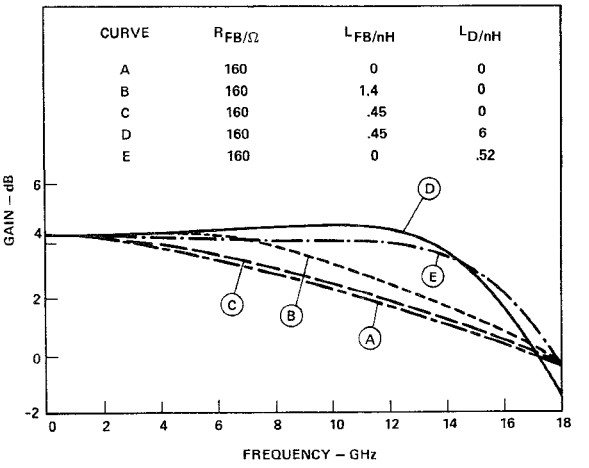

Fig. 2. Computed small-signal gain for various combinations of R_{FB}, L_{FB}, and L_D.

gain response of the basic feedback amplifier. The inductor L_D is mainly responsible for the extended band coverage while the feedback loop provides the flat gain response.

For better understanding of the feedback amplifier's behavior, the vector diagrams of several important voltages as they appear across certain terminals of the amplifier have been drawn at selected frequencies. They are shown in Fig. 3(a) for the case $R_{FB} = 160\ \Omega$, $L_{FB} = 0.45$ nH, $L_D = 0.6$ nH, and in Fig. 3(b) for the case of $R_{FB} = 160\ \Omega$, $L_{FB} = L_D = 0$. All voltages are normalized to $V_S/2$, which is that portion of the source voltage V_S that appears across a 50-Ω load when the signal source is terminated with such a load. Comparing the vector diagrams of Fig. 3 (a) one notices that at 13.75 GHz V_1 and V_2 are in phase, while at very low frequencies they are 180° out of phase. The feedback current I_{FB} has advanced 180° with respect to the signal source current I_S, as is shown in Fig. 4. The signal source current is the current that flows from a 50-Ω source into a 50-Ω load. At 13.75 GHz the ratio V_2/V_1 reaches its maximum and this frequency marks the point of optimum positive feedback.

In order to obtain a more detailed comparison between the behavior of the "conventional negative feedback amplifier" and the amplifier that makes use of controlled feedback, we have plotted the input voltage V_1 and the output voltage V_2 in Fig. 5 as a function of frequency. It can be seen that the influence of L_D and L_{FB} on the magnitude of the input voltage is not very pronounced. Noticeable phase differences exist above 9 GHz, however, with a crossover point at 13.75 GHz. The output voltage of both the conventional negative feedback amplifier and that of the frequency controlled feedback amplifier are almost identical up to 4 GHz. The reactive elements L_D and L_{FB} maintain a nearly constant gain response to almost 14 GHz (curve C) however, which is the reason for the use of reactive control. Also shown in Fig. 5 (curve A) are the input (V_1) and output (V_2) voltages of the amplifier without feedback ($R_{FB} = \infty$). This curve in particular demonstrates the bandwidth potential of the transistor

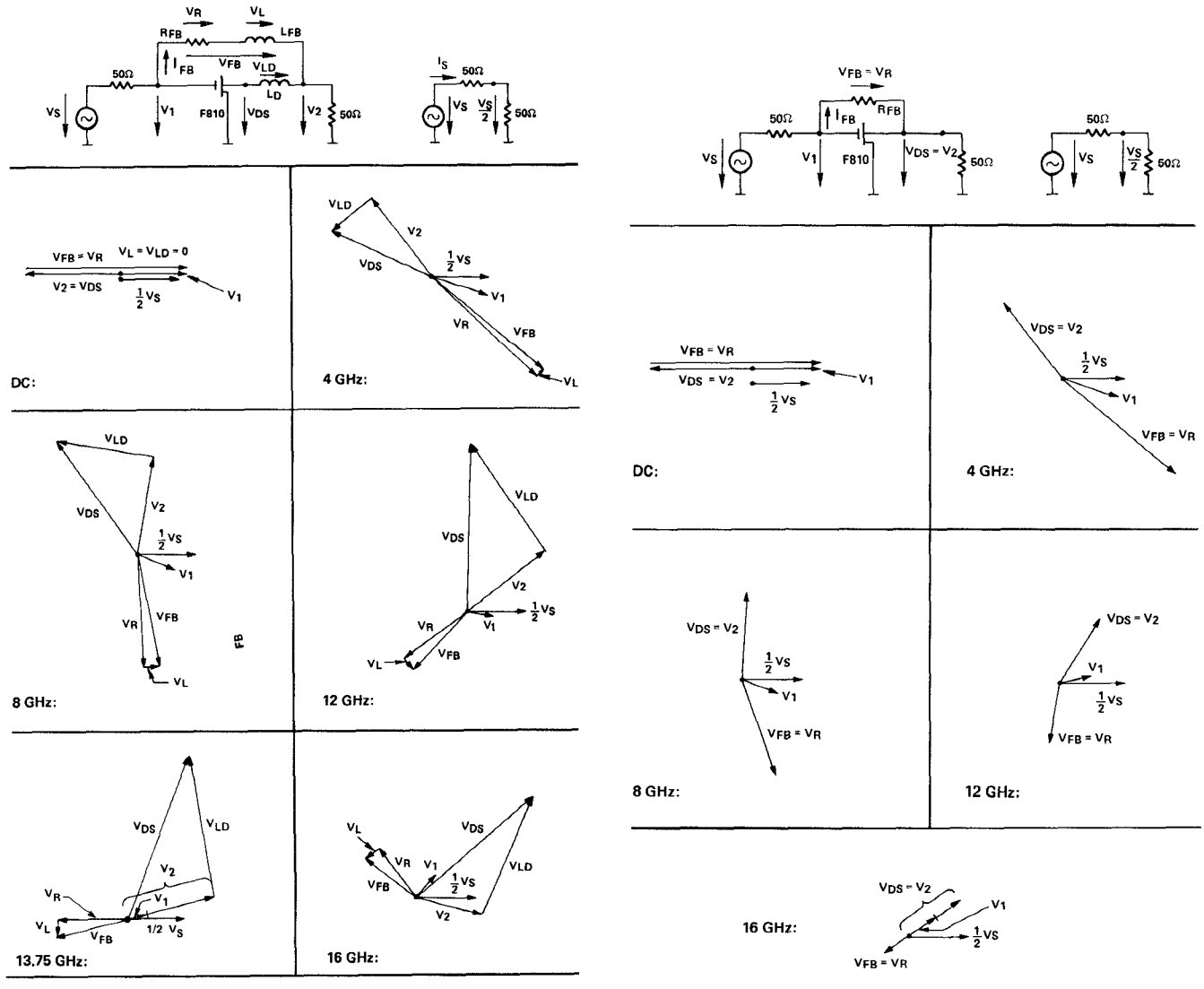

Fig. 3. Voltage vector diagrams of (a) the amplifier with frequency-controlled feedback, and (b) the conventional negative feedback amplifier.

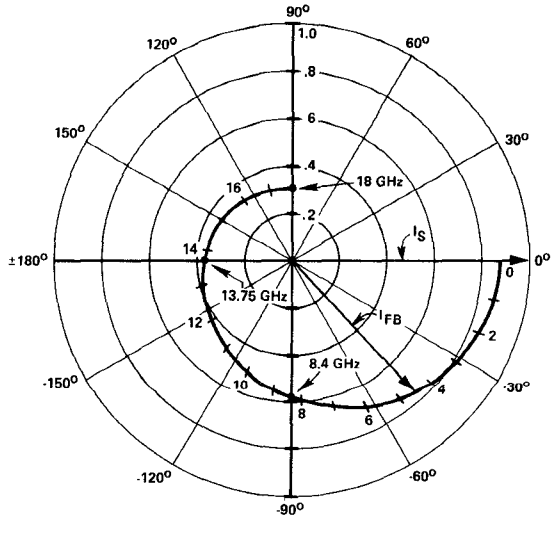

Fig. 4. Magnitude and phase of the normalized feedback current.

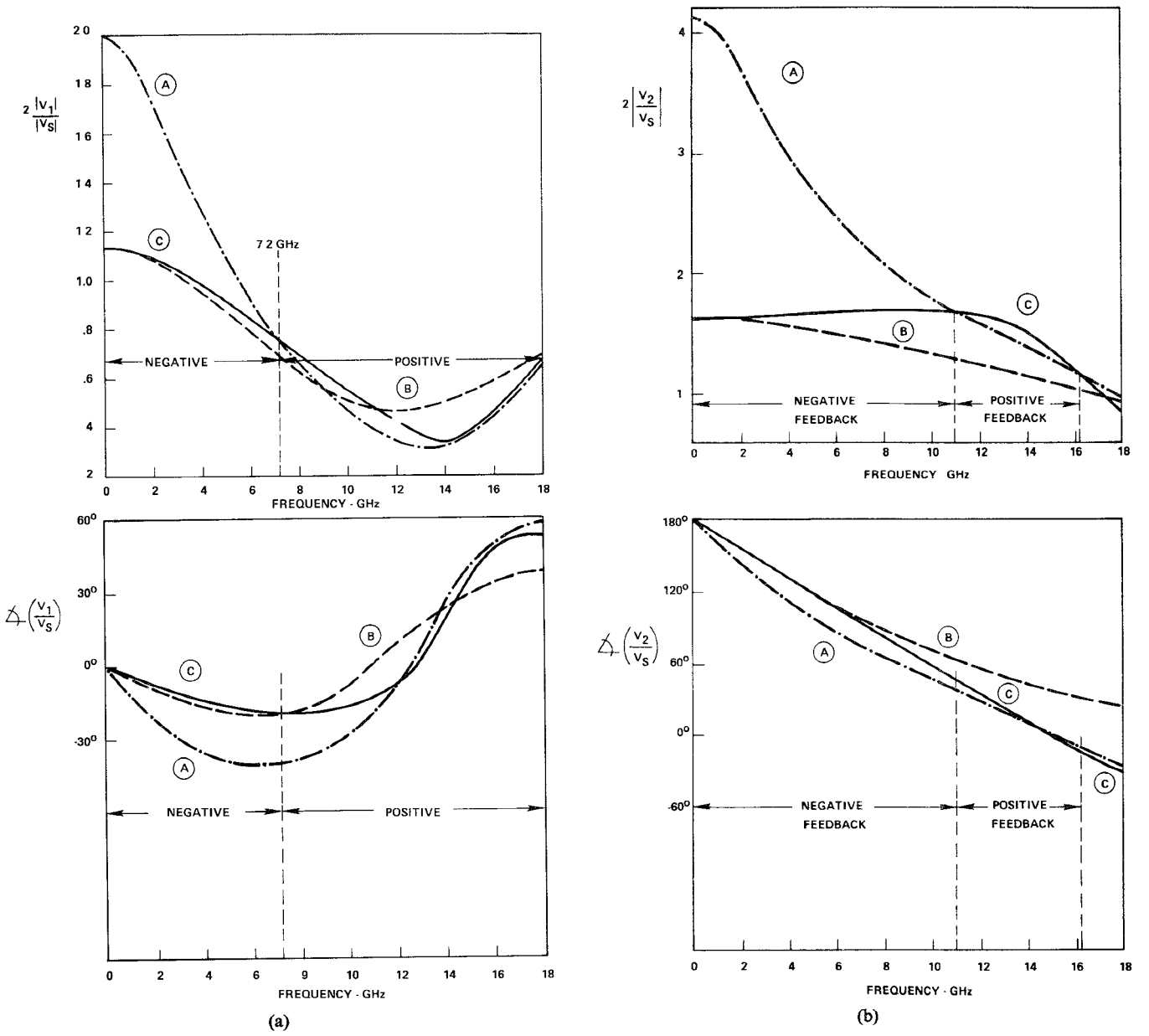

Fig. 5. Normalized input (a) and output (b) voltages. Curve A: the transistor only, $R_{FB}=\infty$; curve B: the conventional negative feedback amplifier, $R_{FB}=160\ \Omega$, $L_{FB}=L_D=0$; curve C: the amplifier with frequency controlled feedback, $R_{FB}=160\ \Omega$, $L_{FB}=0.45$ nH, $L_D=0.6$ nH.

used in our experiments. It also shows the frequency range of positive feedback, i.e., the band in which the feedback elevates the insertion gain above that of the open-loop amplifier (11–16.2 GHz). The feedback loop causes such a "positive range" for the input voltage for all frequencies above 7.2 GHz.

A. Low-Frequency Model

As discussed earlier, the reactive elements of the transistor model under study are relatively low and consequently the circuit diagram of Fig. 1 (a) can be reduced to that of Fig. 1 (b) for frequencies below 1.5 GHz. The usefulness of the low-frequency model is obviously restricted to the very low end of the frequency band. However, the use of the model is justified on the basis that it yields two simple expressions for the feedback resistor R_{FB} ((A.10), (3a)) that we found to be extremely valuable for our amplifier design (see Section IV-A). The model also provides an understanding of the tradeoffs between match and gain. The scattering parameter matrix of the feedback amplifier's low-frequency model (A.4)–(A.9) is derived in its general form in the Appendix. Input and output VSWR become identical if the feedback resistor satisfies the condition (A.10)

For this special case the S parameters are presented in (A.11)–(A.14) of the Appendix. To demonstrate the tradeoff between VSWR and gain, we assume

$$G_{ds}Z_0 \ll 1; \qquad G_{ds} \ll g_m. \tag{1}$$

Using the general set of equations (A.5)–(A.9) of the Appendix, we find the S parameters

$$S_{11}=S_{22}=\frac{1}{\Sigma}\left[\frac{R_{FB}}{Z_0}-g_mZ_0\right] \tag{2a}$$

$$S_{12}=\frac{2}{\Sigma} \tag{2b}$$

$$S_{21}=\frac{-2}{\Sigma}\left[g_mR_{FB}-1\right] \tag{2c}$$

with

$$\Sigma=2+g_mZ_0+\frac{R_{FB}}{Z_0}. \tag{2d}$$

They are plotted in Fig. 6, which shows the relationship between gain, VSWR, transconductance g_m, and feedback resistance R_{FB}. Only the lower section of the right half of the diagram is of practical interest. In this region the amplifier yields the highest-gain–lowest-VSWR combinations. The curves demonstrate that gain at low frequencies can be significantly increased due to an increase of the reflection coefficients. Ideal matching yields the lowest gain. The curves of Fig. 6 further reveal that by varying the feedback resistor the gain can be changed between total attenuation and maximum gain.

The condition for ideal match ($S_{11}=S_{22}=0$) requires

$$R_{FB}=g_mZ_0^2. \tag{3a}$$

The associated gain is

$$G=20\log(g_mZ_0-1). \tag{3b}$$

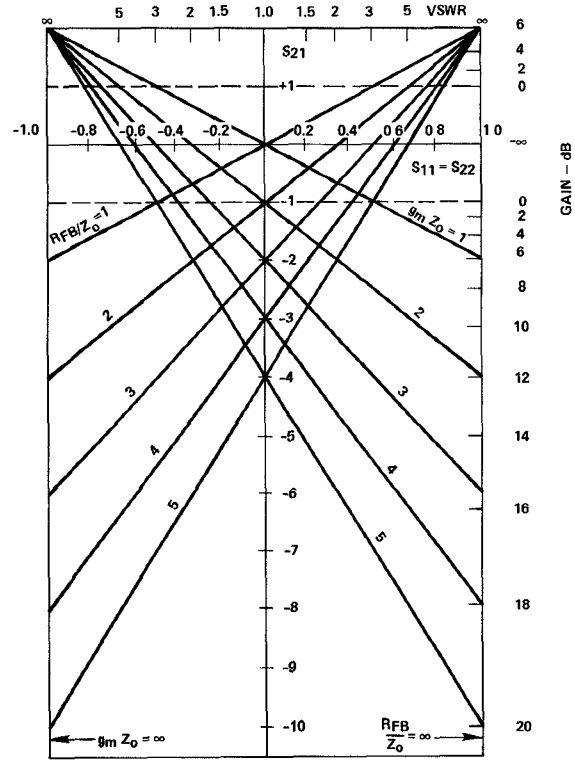

Fig. 6. Gain and VSWR of the low-frequency model for $G_{ds}=0$ and $R_{FB}=g_mZ_0^2$.

C. Circuit Objectives and Requirements

The circuit objective was to extend the bandwidth of the negative feedback amplifier from its upper frequency limit of about 6–14 GHz. The choice of the two series inductances L_D and L_{FB} made this possible. These values were determined as follows.

1) L_D was chosen to compensate for the capacitive component of the GaAs MESFET's output impedance so that resonsance occurs at the upper band edge. This measure simultaneously results in a marked improvement in the output match.

2) L_{FB} was chosen, in cooperation with L_D, to adjust the S parameters of the feedback amplifier so that optimum positive feedback exists at the upper band edge. This condition coincides with the input (V_1) and output (V_2) voltage being in phase and the feedback current I_{FB} advanced by 180° with respect to its phase at very low frequencies. The degree of feedback is mainly controlled by the feedback resistor R_{FB}.

Once steps 1) and 2) are accomplished and the broadband potential of the feedback amplifier shown in Fig. 1(a) is nearly exhausted, a third important step is added; i.e., a simple input and output matching network to further improve the input and output VSWR. In this case one follows published design techniques. Since we chose to use distributed rather than lumped elements, we were confined to short series transmission lines and short open-ended shunt stubs due to the enormous bandwidth we set out to cover. More details on the matching networks will be found in Section IV.

III. Device Technology and Performance

A. Technology

The GaAs MESFET used in this study, the WJ-F810, is the 800-μm gate width device shown in Fig. 7. The chip size is 320 by 370 μm. The 1-μm long gate is centered in a 4-μm source–drain channel.

The GaAs MESFET's were fabricated using a self-aligned etched aluminum gate process described earlier [6]. The n-type active layer was grown by liquid phase epitaxy on Cr-doped substrates The epitaxial layer was doped with Sn to a concentration of 1.0×10^{17} cm^{-3}.

Special emphasis was paid to the reduction of parasitic elements, particularly capacitances which would limit broad-band performance of the transistor. The gate and drain pads were made as small as practical to minimize the input, output, and feedback capacitances. By using 0.5-mil wire for all bond connections we were able to easily bond to these small pads. The minimal size of the source pad is important for other applications which use the common-gate configuration. In this common source application, however, the source pad size is of little concern because both the source pad and the back of the chip are at RF ground. To further minimize the capacitances, a gate–drain spacing of 1.5 μm was chosen, in contrast to 0.9 μm for an earlier device [6]. This spacing is a com-

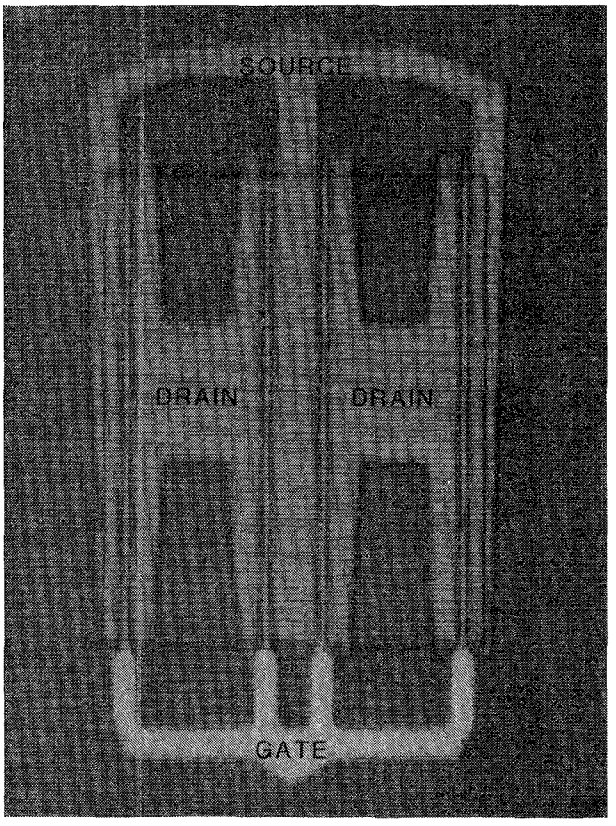

Fig. 7. GaAs MESFET chip (0.32×0.36 mm).

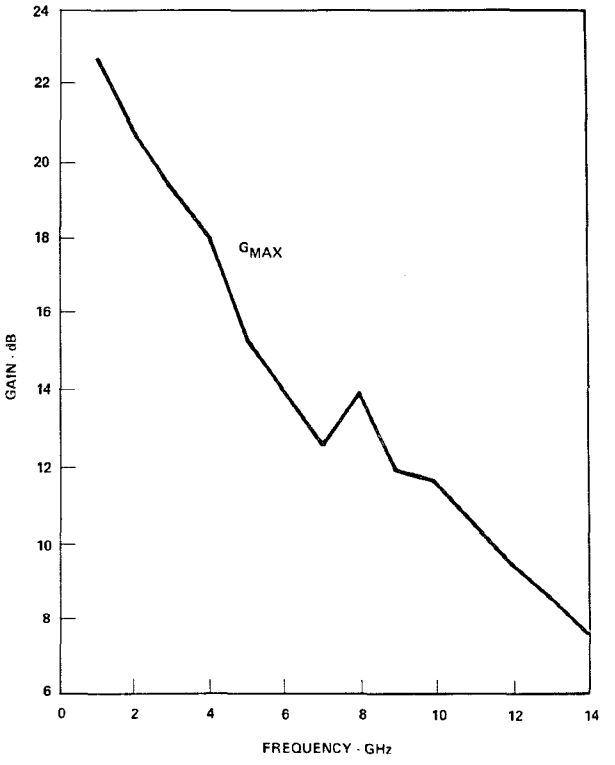

Fig. 8. Measured maximum available gain of the GaAs MESFET.

promise between increased resistance and decreased capacitance.

Most low-noise GaAs FET's have a gate width of about 300 μm. Larger gate widths lead to a linear increase in the transconductance g_m as well as intrinsic capacitances; the cutoff frequency f_t is only slightly affected. The 800-μm gate width was chosen to give substantially higher g_m than available in standard low-noise devices. This high g_m has proven to be an essential element in circuit designs for feedback amplifiers.

B. Transistor Performance and Device Model

The GaAs MESFET has a saturated drain-source current I_{DSS} of 170–240 mA, gate-source pinchoff voltage V_p of 5–7 V, and dc transconductance g_m at $1/2$ I_{DSS} of 50–60 mmhos. The range of the drain-source bias voltage was between 4 and 6 V, depending on output power requirements. Fig. 8 presents the maximum available gain of the device between 1 and 14 GHz.

The device model is shown in Fig. 1 (a) and the quantities of the model elements are given in Table I. The agreement between the measured S parameters and those computed using the model was excellent. Table II compares the parasitic elements of the intrinsic transistor model of the device discussed in this paper with two of our GaAs MESFET's which have been described elsewhere ([6], [7]). The element values are normalized to the gate width for reasons of comparison. It can be seen that the topology of the WJ-F810 has lead to a significant reduction in the magnitudes of the normalized capacitive elements making this device highly suitable for broadband applications.

TABLE II
ELEMENTS OF TRANSISTOR MODELS NORMALIZED TO GATEWIDTH

PARAMETER	UNIT	WJ-F110	WJ-F1010	WJ-F810
W_{GATE}	μm	300	1000	800
L_{GATE}	μm	1	1	1
g_m/W	mmhos/mm	73	68	68
C_{gs}/W	pF/mm	1.37	.94	.84
C_{gd}/W	pF/mm	.033	.055	.021
C_{dc}/W	pF/mm	.097	.047	.040
C_{ds}/W	pF/mm	.41	.24	.10

IV. AMPLIFIER DESIGN AND PERFORMANCE

A. Small-Signal Design

The first step in designing an ultrabroad-band feedback amplifier is the selection of the feedback resistor R_{FB}. According to Table I the transconductance g_m and the drain-source conductance G_{ds} of our device are 0.054 mhos and 0.005 mho, respectively. If it is desired that input and output VSWR be identical, we find from (A10)–(A14) that, at very low frequencies, a gain of 4.2 dB and an input and output VSWR of 1.2:1 will be obtained for $R_{FB}=(g_m+G_{ds})Z_0^2=147.5$ Ω. Raising the

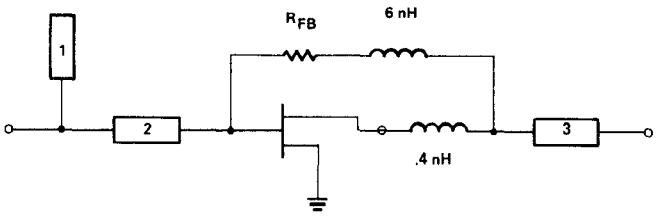

ELEMENT	IMPEDANCE (Ω)	LENGTH AT 8 GHz
NO. 1	25	14.3°
NO. 2	55	18.0°
NO. 3	75	10.0°

(a)

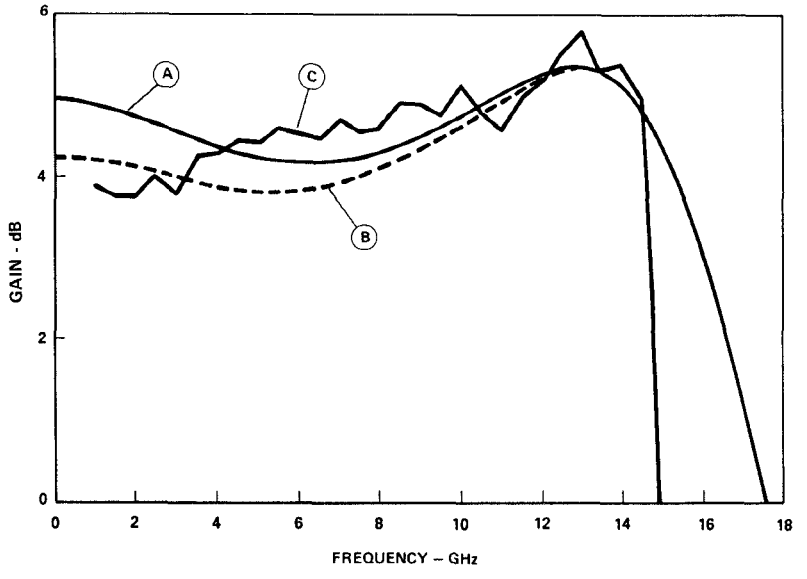

(b)

Fig. 9. Schematic (a) and gain curves (b) of the matched feedback amplifier. Curve *A*: computed for $R_{FB}=180\ \Omega$; curve *B*: computed for $R_{FB}=160\ \Omega$; curve *C*: measured for $R_{FB}=160\ \Omega$ ($V_{DS}=4$ V, $I_{DS}=53$ mA).

feedback resistor to $R_{FB}=160\ \Omega$ increases the gain to 4.6 dB as calculated with (A.7). Using (A.5) and (A.8) the input VSWR for this case computes to 1.27:1 and the output VSWR to 1.13:1.

The selection of L_D and L_{FB} as well as the influence of these two inductors on gain has been described in detail in Section II. The gain response of the basic feedback amplifier shown in Fig. 1 (a) with $R_{FB}=160\ \Omega$ is nearly flat to almost 14 GHz (Fig. 2, curve *D*). However, the corresponding input reflection coefficient is rather poor above 8 GHz. In order to improve the input match over the upper portion of the band, we employed an open-circuit shunt stub and a series transmission line. Due to the feedback, these two components had a negative influence on the output match, so we inserted a series transmission line connected to the output terminal of the basic amplifier to counteract the degradation of the output reflection coefficient. The introduction of the input and output matching networks led to the matched feedback amplifier.

The schematic of the matched feedback amplifier is shown in Fig. 9 (a). The selection of $L_{FB}=0.6$ nH and $L_D=0.4$ nH deviates from the optimum values of $L_{FB}=0.45$ nH and $L_D=0.6$ nH discussed in Section II. This change was made to attain a more practical circuit layout. Since L_{FB} bridges most of the physical distance between the transistor's gate terminal and the node between L_D and the series transmission line, it becomes somewhat impractical to make L_{FB} smaller than L_D. In addition, a higher feedback resistor of $R_{FB}=180\ \Omega$ was inserted to obtain optimum gain flatness for the new set of inductors. These measures constitute a necessary tradeoff between practicality and optimum performance. The computed small signal gain of the amplifier between 50-Ω impedances is plotted as curve *A* of Fig. 9 (b), while curve *B* represents the computed small signal gain for $R_{FB}=160\ \Omega$. The computed reflection coefficients of the practical version of the matched amplifier (Fig. 9 (a)), the negative feedback amplifier (Fig. 3 (b)), and the basic feedback amplifier (Fig. 3 (a)) are plotted in Fig. 10 as curves *A*, *B*,

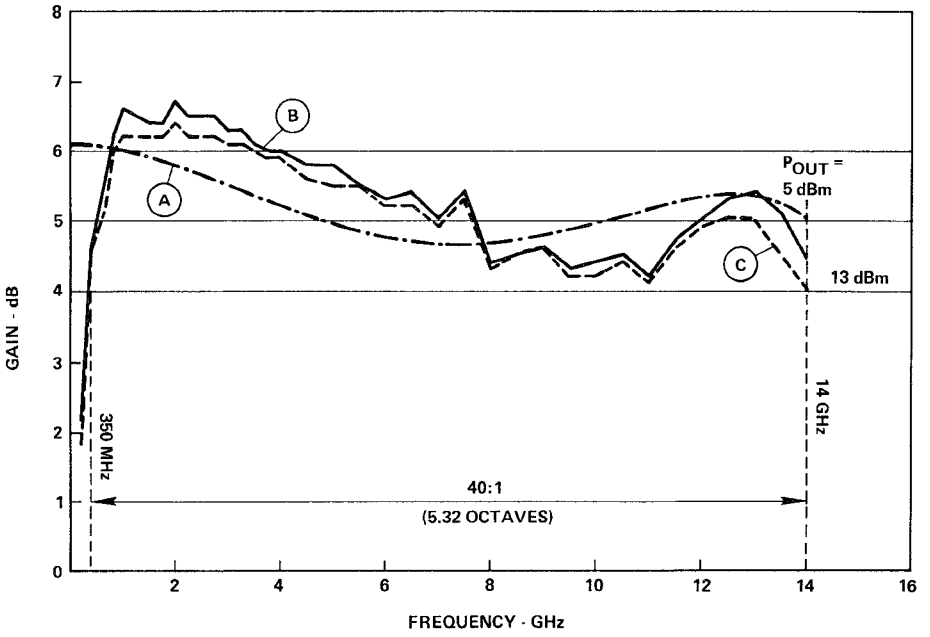

Fig. 10. Input and output reflection coefficients. Curve A: matched feedback amplifier of Fig. 9 (a) with $R_{FB}=180\ \Omega$, $L_{FB}=0.6$ nH, $L_D=0.4$ nH; curve B: conventional negative feedback amplifier of Fig. 3 (b) with $R_{FB}=160\ \Omega$, $L_{FB}=L_D=0$; curve C: basic feedback amplifier of Fig. 3 (a) with $R_{FB}=160\ \Omega$, $L_{FB}=0.45$ nH, $L_D=0.6$ nH.

and C, respectively. The input reflection coefficient of the matched amplifier shows a significant improvement brought about by the matching circuits.

However, the output reflection coefficient has experienced a slight degradation due to the influence of the input matching circuit on the output impedance brought about by the feedback loop. This is particularly pronounced in the area of relatively strong feedback, i.e., above 11 GHz. The amplifier is unconditionally stable up to 13.8 GHz. Reverse isolation computed between dc and 18 GHz has a minimum value of 9.7 dB at 17 GHz for $R_{FB}=160\ \Omega$ and 10 dB at 16 GHz for $R_{FB}=180\ \Omega$.

B. Amplifier Fabrication and Performance

Fused silica, 0.015 in in thickness, was used as substrate material for the input and output circuits. The circuit pattern was etched into a thin gold film, while the feedback resistor was subsequently etched into a tantalum nitride film which was deposited below the gold.

The measured small-signal gain of the amplifier is plotted in Fig. 9 (b) (curve C). The feedback resistor of this unit measured $R_{FB}=160\ \Omega$ instead of the desired 180 Ω. A comparison of the measured small-signal gain and the gain computed for $R_{FB}=160\ \Omega$ (curve B) shows excellent agreement at frequencies up to 14.5 GHz. Beyond this frequency the actual measured gain dropped rather abruptly. Below 1 GHz the drop in gain was due to the influence of the internal dc biasing network (not shown in the schematic of Fig. 9 (a)). The measured reverse isolation had its minimum value of $|S_{12}|^2_{\min}=14$ dB at 1 GHz. This isolation is somewhat better than the 11.2 dB computed with (A.6). Maximum measured reverse isolation was $|S_{12}|^2_{\max}=21$ dB at 10.5 GHz which compares to the maximum computed value of 22.4 dB at 9 GHz. The reflection coefficients of the actual amplifier did not exceed $|S_{11}|_{\max}=0.38$ for the input and $|S_{22}|_{\max}=0.37$ for the output terminal between 2 GHz and 14.4 GHz. The computed values were $|S_{11}|_{\max}=0.42$ and $|S_{22}|_{\max}=0.37$, respectively.

The measured small-signal gain of an identical amplifier module except for $R_{FB}=225\ \Omega$ is plotted as curve B in Fig. 11. Biasing of this amplifier was accomplished by means of external bias networks. The drop in the measured gain below 1 GHz was caused by the 50-pF dc blocking capacitor in the feedback loop and by the bias networks. The capacitor serves the purpose of separating the drain bias from the gate bias potential. The computed gain is plotted as curve A, while curve C shows the gain at 13 dBm of output power. This module covers a 40:1 bandwidth ranging from 350 MHz to 14 GHz, or almost 5 1/3 octaves. Maximum input and output reflection coefficients between 350 MHz and 14 GHz were $|S_{11}|_{\max}=0.45$ and $|S_{22}|_{\max}=0.54$, respectively. A minimum reverse isolation of $|S_{12}|^2_{\min}=11.5$ dB was measured at 14 GHz. Computed and measured reflection coefficients and minimum reverse isolations are in good agreement.

V. Conclusion

The design of an ultrawide-band amplifier has been described which makes use of both negative and positive feedback. The frequency dependence of the feedback is controlled by two inductors, one in series with the feed-

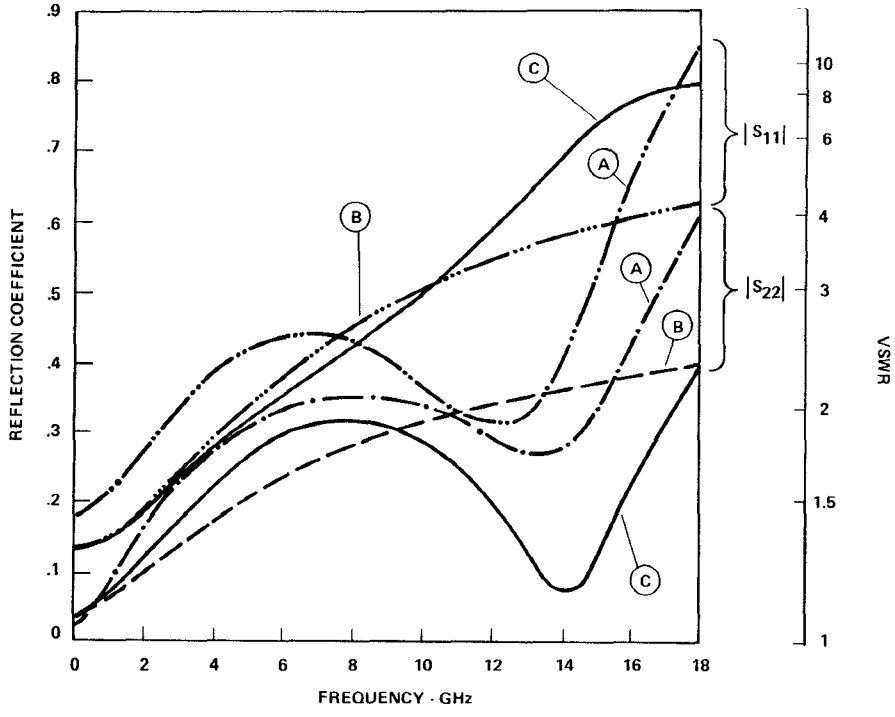

Fig. 11. Gain of the matched feedback amplifier for $R_{FB}=225\ \Omega$. Curve *A*: computed small signal gain; curve *B*: measured gain at 5 dBm of output power ($V_{DS}=5$ V, $I_{DS}=72$ mA); curve *C*: measured gain at 13 dBm of output power ($V_{DS}=5$ V, $I_{DS}=72$ mA).

back resistor and the other in series with the output of the GaAs MESFET. A detailed study of the effect of the inductors on the characteristics of the feedback amplifier has been made and guidelines have been presented on how to determine their magnitudes. In addition to the feedback circuitry, simple matching networks have been employed to improve the input and output reflection coefficients. The GaAs MESFET used in the experiments was designed with major emphasis on reducing its parasitics. These efforts resulted in a device with ultrawide bandwidth capability.

Two experimental amplifier modules have been described that cover the frequency band 1.0–14.5 GHz and 350 MHz–14.0 GHz with 3.8 dB and 4.2 dB of minimum gain, respectively. Maximum reflection coefficients of these single-ended units were $|S_{11}|_{\max}=0.38$ and $|S_{11}|_{\max}=0.45$ for the respective input terminals and $|S_{22}|_{\max}=0.37$ and $|S_{22}|_{\max}=0.54$ for the respective output terminals. Minimum reverse isolations across these bands were $|S_{12}|^2_{\min}=14$ dB and $|S_{12}|^2_{\min}=11.5$ dB, respectively. The agreement between the computed and the measured data of small-signal gain, reflection coefficients, and reverse isolation was very good.

The use of the matched feedback amplifier with GaAs MESFET's provides several advantages over usual techniques for broad-band microwave amplification. It has an exceptionally wide bandwidth and much lower reflection coefficients than regular single-ended amplifiers of comparable bandwidths. It can be constructed with a very simple and small circuit and is relatively easy to cascade. These advantages make feedback amplifiers prime candidates for monolithic applications.

Appendix

The equivalent circuit of a GaAs MESFET feedback amplifier as shown in Fig. 1 (a) can be reduced to the model of Fig. 1 (b) for frequencies at which the reactive elements of the transistor and the matching networks may be neglected. A discussion of the limitations of the low-frequency model is found in Section II.2. Under these conditions and the assumption that R_d and R_s of Fig. 1 (a) are very small compared to the feedback resistor R_{FB} and the load resistor $R_L=Z_0$ voltages and currents are described by the simple conductance matrix

$$\begin{bmatrix} I_1 \\ I_2 \end{bmatrix} = \begin{bmatrix} G_{FB} & -G_{FB} \\ (g_m - G_{FB}) & (G_{FB}+G_{ds}) \end{bmatrix} \begin{bmatrix} V_1 \\ V_2 \end{bmatrix} \quad \text{(A.1)}$$

where

$$G_{FB}=R_{FB}^{-1} \quad \text{(A.2a)}$$

$$G_{ds}=R_{ds}^{-1} \quad \text{(A.2b)}$$

and

$$i_{gs}=g_m V_{gs}. \quad \text{(A.3)}$$

Using elementary algebra, the matrix (A.1) converts into the scattering parameter matrix

$$S_{ij}=\begin{bmatrix} S_{11} & S_{12} \\ S_{21} & S_{22} \end{bmatrix}. \quad \text{(A.4)}$$

Its elements are

$$S_{11}=\frac{1}{\Sigma}\left[\frac{R_{FB}}{Z_0}(1+G_{ds}Z_0)-(g_m+G_{ds})Z_0\right] \quad (A.5)$$

$$S_{12}=\frac{2}{\Sigma} \quad (A.6)$$

$$S_{21}=\frac{-2}{\Sigma}\left[g_m R_{FB}-1\right] \quad (A.7)$$

$$S_{22}=\frac{1}{\Sigma}\left[\frac{R_{FB}}{Z_0}(1-G_{ds}Z_0)-(g_m+G_{ds})Z_0\right] \quad (A.8)$$

with

$$\Sigma=2+(g_m+G_{ds})Z_0+\frac{R_{FB}}{Z_0}(1+G_{ds}Z_0). \quad (A.9)$$

For the condition

$$\frac{R_{FB}}{Z_0}=(g_m+G_{ds})Z_0 \quad (A.10)$$

we find

$$S_{11}=-S_{22}=\frac{G_{ds}Z_0^2}{\Sigma}(g_m+G_{ds}) \quad (A.11)$$

$$S_{12}=\frac{2}{\Sigma} \quad (A.12)$$

$$S_{21}=-\frac{2}{\Sigma}\left[g_m(g_m+G_{ds})Z_0^2-1\right] \quad (A.13)$$

$$\Sigma=2+(g_m+G_{ds})(2+G_{ds}Z_0)Z_0. \quad (A.14)$$

The reflection coefficients S_{11} and S_{22} improve with decreasing drain-source conductance G_{ds}. The general (A.5)–(A.9) and the special (A.10)–(A.14) equations for the S parameters demonstrate that gain, input and output VSWR, and reverse isolation are all fixed quantities once the value for the feedback resistor R_{FB} is chosen.

The ideal matching condition

$$S_{11}=S_{22}=0 \quad (A.15)$$

can only be satisfied for

$$G_{ds}=0$$

and

$$\frac{R_{FB}}{Z_0}=g_m Z_0. \quad (A.16)$$

In this case we find the S parameters

$$S_{11}=S_{22}=0 \quad (A.17)$$

$$S_{12}=\frac{1}{g_m Z_0+1} \quad (A.18)$$

$$S_{21}=-(g_m Z_0-1). \quad (A.19)$$

ACKNOWLEDGMENT

The authors wish to thank R. Pereira, who was responsible for the measurement and the tuning of the amplifiers. Thanks are also due to A. Hallin, K. Lutz, and K. Lindstedt, who fabricated the GaAs MESFET devices and to J. Martin, who assembled the circuits. The authors are indebted to S. Rose, who was responsible for device testing, and to M. Walker for many helpful discussions.

REFERENCES

[1] H. S. Black, "Stabilized feedback amplifiers," *Elec. Eng.*, vol. 53, pp. 114–120, Jan. 1934.
[2] F. E. Terman, *Radio Engineer's Handbook*. New York: McGraw-Hill, 1943, pp. 395–406.
[3] M. S. Ghausi, *Principles and Designs of Linear Active Circuits*. New York: McGraw-Hill, 1965, pp. 363–370.
[4] E. Ulrich, "Use of negative feedback to slash wideband VSWR," *Microwaves*, pp. 66–70, Oct. 1978.
[5] R. Dawson, "Equivalent Circuit of the Schottky-barrier field-effect transistor at microwave frequencies," *IEEE Trans. Microwave Theory Tech.*, vol. MTT-23, pp. 499–501, June 1975.
[6] K. B. Niclas, R. B. Gold, W. T. Wilser, and W. R. Hitchens, "A 12-18 GHz medium power GaAs MESFET amplifier," *IEEE J. Solid State Circuits*, vol. SC-13, pp. 520–527, Aug. 1978.
[7] K. B. Niclas, W. T. Wilser, R. B. Gold, and W. R. Hitchens, "Application of the two-way balanced amplifier concept to wideband power amplification using GaAs MESFET's," *IEEE Trans. Microwave Theory Tech.*, to be published.